Journal of Orthopaedic Translation 38 (2023) 98–105

Contents lists available at ScienceDirect

Journal of Orthopaedic Translation

journal homepage: www.journals.elsevier.com/journal-of-orthopaedic-translation

MLK3 silence suppressed osteogenic differentiation and delayed bone formation via influencing the bone metabolism and disturbing MAPK signaling

Xiao Yang [a,1], Yong-xin Mai [b,c,1], Lan Wei [b,d], Li-yang Peng [b,c], Feng-xiang Pang [b,c], Ling-jun Wang [b,d], Zhi-peng Li [b,c,e,***], Jin-fang Zhang [b,c,*], An-min Jin [a,**]

[a] Department of Spinal Surgery, Zhujiang Hospital, Southern Medical University, Guangzhou, China
[b] Lingnan Medical Research Center, Guangzhou University of Chinese Medicine, Guangzhou, China
[c] Key Laboratory of Orthopaedics and Traumatology, The First Affiliated Hospital of Guangzhou University of Chinese Medicine, The First Clinical Medical College, Guangzhou University of Chinese Medicine, Guangzhou, China
[d] The First Affiliated Hospital, Guangzhou University of Chinese Medicine, Guangzhou, China
[e] Department of Rehabilitation, The Sixth Affiliated Hospital, Sun Yat-sen University, Guangzhou, China

ARTICLE INFO

Keywords:
MLK3
Bone formation
Bone metabolism
Fracture
Fracture healing

ABSTRACT

Background: Mixed lineage kinase 3 (MLK3) is a member of a serine/threonine MAP3K family, and it has been demonstrated to play critical roles in various biological activities and disease progression. Previous studies showed that impaired skeletal mineralization and spontaneous tooth fracture in the MLK3-deficient mice, suggesting MLK3 actively participated in the bone formation. However, the detailed function and underlying mechanisms remain obscure.

Methods: The MLK3 knockout (KO) mouse was applied in the present study, and multi-omics were performed to compare the metabolites and gene expression between wild type (WT) and KO mice. The bone fracture model was successfully established, and the healing process was evaluated by X-ray, micro-CT examination, histomorphometry and immunohistochemistry (IHC) staining. On the other hand, the effects of MLK3 on osteogenic differentiation were assessed by alkaline phosphatase (ALP) activity, Alizarin red S (ARS) staining and qRT-PCR examination. Finally, the downstream signaling pathways were screened out by RNA-sequencing (RNA-seq) and then validated by Western blotting.

Results: In the present study, imbalanced bone metabolism was observed in these MLK3 KO mice, suggesting MLK3 may participate in bone development. Moreover, MLK3 −/− mice displayed abnormal bone tissues, impaired bone quality, and delayed fracture healing. Further investigation showed that the inhibition of MLK3 attenuated osteoblast differentiation *in vitro*. According to the RNA-seq data, MAPK signaling was screened out to be a downstream pathway, and its subfamily members extracellular signal-regulated kinase (ERK), p38 and Jun N-terminal protein kinase (JNK) were subjected to Western blotting examination. The results revealed that although no differences in their expression were observed between MSCs derived from WT and KO mice, their phosphorylated protein levels were all suppressed in MLK3 −/− MSCs.

Conclusion: In conclusion, our results demonstrated that loss of MLK3 suppressed osteoblast differentiation and delayed bone formation via influencing metabolism and disturbing MAPK signaling.

The translational potential of this article: The findings based on the current study demonstrated that MLK3 promoted osteogenesis, stimulated new bone formation and facilitated fracture healing, suggesting that MLK3 may serve as a potential therapeutic target for bone regeneration. MLK3 activator therefore may be developed as a therapeutic strategy for bone fracture.

* Corresponding author. Department of Spinal Surgery, Zhujiang Hospital, Southern Medical University, Guangzhou, China. Tel: +86 13802983267.
** Corresponding author. Lingnan Medical Research Center, Guangzhou University of Chinese Medicine, Guangzhou, China.
*** Corresponding author. Lingnan Medical Research Center, Guangzhou University of Chinese Medicine, Guangzhou, China. Tel: +86 13724839892.
E-mail addresses: Dr.LiZhipeng@gmail.com (Z.-p. Li), zhangjf06@gzucm.edu.cn (J.-f. Zhang), jinanmin2008@163.com (A.-m. Jin).
[1] Yang X. and Mai Y.X. contributed equally to this paper.

https://doi.org/10.1016/j.jot.2022.07.003
Received 28 March 2022; Received in revised form 21 June 2022; Accepted 5 July 2022

2214-031X/© 2022 Published by Elsevier B.V. on behalf of Chinese Speaking Orthopaedic Society. This is an open access article under the CC BY-NC-ND license (http://creativecommons.org/licenses/by-nc-nd/4.0/).

1. Introduction

As a common orthopedic disease, the fracture is caused by many factors such as trauma, inflammation, tumor, diabetes and osteoporosis [1–3]. It can seriously threaten the quality of life and workability of patients, and bring a heavy burden to the family and society [4,5]. According to the survey in healthcare epidemiology, most people in developed countries may experience at least one fracture during their lifetime [6]. The clinical therapeutics for bone fracture is mature, and surgery is a common intervention in clinical practice [7]. However, the fractured bone needs a long time to recover, and even about 5%–10% of fracture patients remain delayed union or nonunion [8,9]. The delayed union and nonunion in elderly patients are more common due to the poor proliferation and differentiation potential of their mesenchymal progenitor cells [6]. Therefore, how to promote the potential of osteoblast differentiation is of great clinical significance for bone fracture.

Mixed lineage kinase 3 (MLK3), also known as MAP3K11, is a member of a serine/threonine MAP3K family [10,11]. As a member of the kinase family, it contains a kinase catalytic domain with sequence similarity to both serine/threonine and tyrosine kinases, and it can activate mitogen-activated protein kinase (MAPK) signaling pathways such as Jun N-terminal protein kinase (JNK), p38 and extracellular signal-regulated kinase (ERK) [10–13]. As an activator of MAPK signaling, MLK3 plays an essential role in various biological activities and disease progression such as tumorigenesis, inflammation, metabolic dysfunction, etc [14–19]. Interestingly, impaired skeletal mineralization has been reported in MLK3 deficient mice, and the spontaneous tooth fracture has also been reported in the MLK3 knockout (KO) mice [12]. Notably, Mlk3 −/− mice had similar numbers of osteoclasts *in vivo*, and MLK3 absence had any influence on osteoclast differentiation capacity [12]. These observations suggest further investigation into the link between MLK3 and osteoblasts would likely yield new insights into developing a potential therapeutic target for bone fracture.

In the present study, the MLK3 KO mice were generated and the multi-omics analyses revealed the imbalanced bone metabolism in these KO mice. These KO mice exhibited abnormal bone tissues, impaired bone quality and a delayed fracture healing. Moreover, MLK3 inhibitor URMC-099 suppressed the osteoblast differentiation *in vitro*. Further mechanistic studies discovered that MAPK signaling, including JNK, p38 and ERK, were suppressed after the inhibition of MLK3. Taken together, MLK3 was considered to promote osteogenesis, stimulate bone formation and facilitate fracture healing, suggesting that it may be a potential therapeutic target for bone repair.

2. Materials and methods

2.1. Animals

The MLK3 gene KO (-/-) mice were kindly provided by Prof. Ling-jun Wang (Lingnan Medical Research Center, Guangzhou University of Chinese Medicine). Tamoxifen was administrated to achieve gene absence at a specific time. This study was approved by the Institutional Animal Care and Use Committee (IACUC) of Guangzhou University of Chinese Medicine (Guangzhou, China).

2.2. Metabonomics and transcriptomics

The metabolomics and transcriptomics were performed by the Shanghai luming biological technology Co., Ltd. Briefly, 12-week-old wide type (WT) and KO mice were sacrificed, and the cleaned femurs were provided for the untargeted and Gas chromatography-mass spectrometry (GC–MS) based metabolomics was carried out using an Agilent 7890 B gas chromatography system combined with a 5977 B MSD system (Agilent Technologies Inc., CA, USA). As for the transcriptomics, the cortical bone of femurs were isolated, frozen by liquid nitrogen and ground to generate RNA for transcriptome profiling. The metabolites and genes were analyzed, and then a heat map and volcano plot were performed using R3.6.3. Gene set enrichment analysis (GSEA) was conducted to identify the enriched signaling.

2.3. Cell culture and osteogenic induction

The mouse mesenchymal stem cells (MSCs) were isolated from the bone marrow of 12-week-old KO and WT mice. Their bone marrows were flushed out, and the cells were maintained in Dulbecco's modified Eagle medium (DMEM) supplemented with 10% FBS and 1% penicillin/streptomycin. The culture was kept in a humidified 5% CO2 incubator at 37 °C. After several passages, MSCs were identified using flow cytometry and induced osteogenesis differentiation with the classical inducers, including 10 nM dexamethasone (Sigma–Aldrich, St. Louis, MO, USA), 50 μg/ml ascorbic acid (Sigma–Aldrich), and 10 mM glycerol 2-phosphate (Sigma–Aldrich). The osteogenic induction medium was changed every three days.

2.4. Cell viability

MSCs were seeded in 96-well microplates and treated with various concentrations of URMC-099 for 24, 48, 72 and 96 h. Then cells viability was determined by CCK8 examination (Cell Counting Kit 8, Beyotime, Shanghai, China) and measured at OD 450 nm with the Microplate Reader (Multiskan GO, Thermo Fisher Scientific, Finland).

2.5. Alkaline phosphatase (ALP) activity and alizarin red S (ARS) staining

The osteoblast differentiation was induced, and the ALP activity and ARS staining were examined at designated time points. Briefly, the cells were harvested by cell scratch, and ALP activity was measured by ALP staining. As for ARS analyses, the cells were washed and fixed with 70% ethanol for 30min, then stained with 2% ARS solution for 10min. The stained calcified nodules were scanned using UMAX Powerlook 1120xl (Amersham biosciences, Canon, Japan).

2.6. RNA extraction and quantitative polymerase chain reaction (qPCR) examination

Total RNA were extracted by TRIzol reagent (15596026, Invitrogen), and their concentration was measured by Nanodrop (Thermo Fisher Scientific). Subsequently, cDNA was reversely transcribed by PrimeScript RT Master Mix (TaKaRa, Japan). Then, the qRT-PCR examination was conducted using the PowerUp™ SYBR™ Green Master Mix (Thermo Fisher Scientific) on the LightCycler 480 system (Roche, Basel, Switzerland). The relative fold changes of candidate genes were calculated by using the $2^{-\Delta\Delta Ct}$ method. Primer sequences used in this examination were listed in Table 1.

2.7. Western blotting

Total protein was extracted from the MSCs derived from KO and WT mice by Cell lysis buffer (Beyotime, Shanghai, China) and qualified by the BCA assay kit (Thermo Fisher Scientific). Then the soluble protein was separated by SDS-PAGE (10%) and transferred to PVDF membranes. The membranes were then blocked with 5% skimmed milk and probed with the corresponding antibody: JNK (1:1000; Proteintech, USA), p-JNK (1:1000; Cell Signaling Technology, USA), p-P38 (1:1000; Cell Signaling Technology, USA), ERK (1:1000; Cell Signaling Technology, USA), p-ERK (1:1000; Proteintech, USA), GADPH (1:1000; Cell Signaling Technology, USA). After incubation with the appropriate secondary antibody, the chemiluminescence (ECL, Hangzhou, China) was applied to visualize the bands.

Table 1
Primers for qRT-PCR examination.

	Forward	Reverse
OSX	GTGAATTCACCTTTCAGCCCCAAAACC	TGGGATCCCAGCTGTGAATGGGCTTCTT
RUNX2	GACTGTGGTTACCGTCATGGC	ACTTGGTTTTTCATAACAGCGGA
OCN	GCAGGAGGGCAATAAGGT	CGTAGATGCGTTTGTAGGC□□
ALP	GCCCTCTCCAAGACATATA	CCATGATCACGTCGATATCC
OPN	TCACCATTCGGATGAGTCTG	ACTTGTGGCTCTGATGTTCC
BMP2	AGTTCTGTCCCCAGTGACGAGTTT	GTACAACATGGAGATTGCGCTGAG
18 S	TGGTTGCAAAGCTGAAACTTAAAG	AGTCAAATTAAGCCGCAGGC

2.8. Animal femoral fracture model

The modified mice closed transverse femoral fracture model was established in this study [20]. Briefly, this surgery was carried out under general anesthesia (1% pentobarbital sodium, intraperitoneal injection, 8ul/g) and in sterile condition. A 1 cm incision was made in the lateral aspect of the right thigh, and the osteotomy was made with an electric saw at the middle site of the femur. Then the femur was fixed with a gauge 30 needle penetrated into the medullary cavity. At week 4 and week 6 post-surgery, X-ray radiography was taken to determine the status of fracture healing.

2.9. Micro-computer tomography (μCT) scanning

The μCT analyses were performed using a high-resolution μCT instrument (SkyScan1172, Bruker, German). The samples were inversely placed in a 12 mm diameter scanning holder and scanned at the following settings: a source voltage of 70 keV, current of 80 μA, power of 7 W, 4 frames superimposed, angle gain of 0.72°, exposure time of 100 ms and 10 μm isotropic resolution. When the fractured bones were evaluated, 2.5 mm diameter around the center of the fracture line and 1 mm below the center was defined as the region of interest (ROI) for the analysis. When the normal bone tissues were analyzed, the ROI was defined as 0.7 mm away from the growth plate and 1.5 mm long trabecular bone. The three dimensional (3D) reconstruction was performed using μCT Ray v.3.8, and the trabecular bone volume (BV), total volume (TV), trabecular bone surface (BS), total surface (TS), BV/TV, BS/BV, BS/TV, trabecular bone thickness (Tb.Th), trabecular bone number (Tb.N), trabecular bone separation (Tb.Sp), bone mineral density (BMD) were recorded for quantitative calculation using the CT-VOX software (CtAN, Bruker, German).

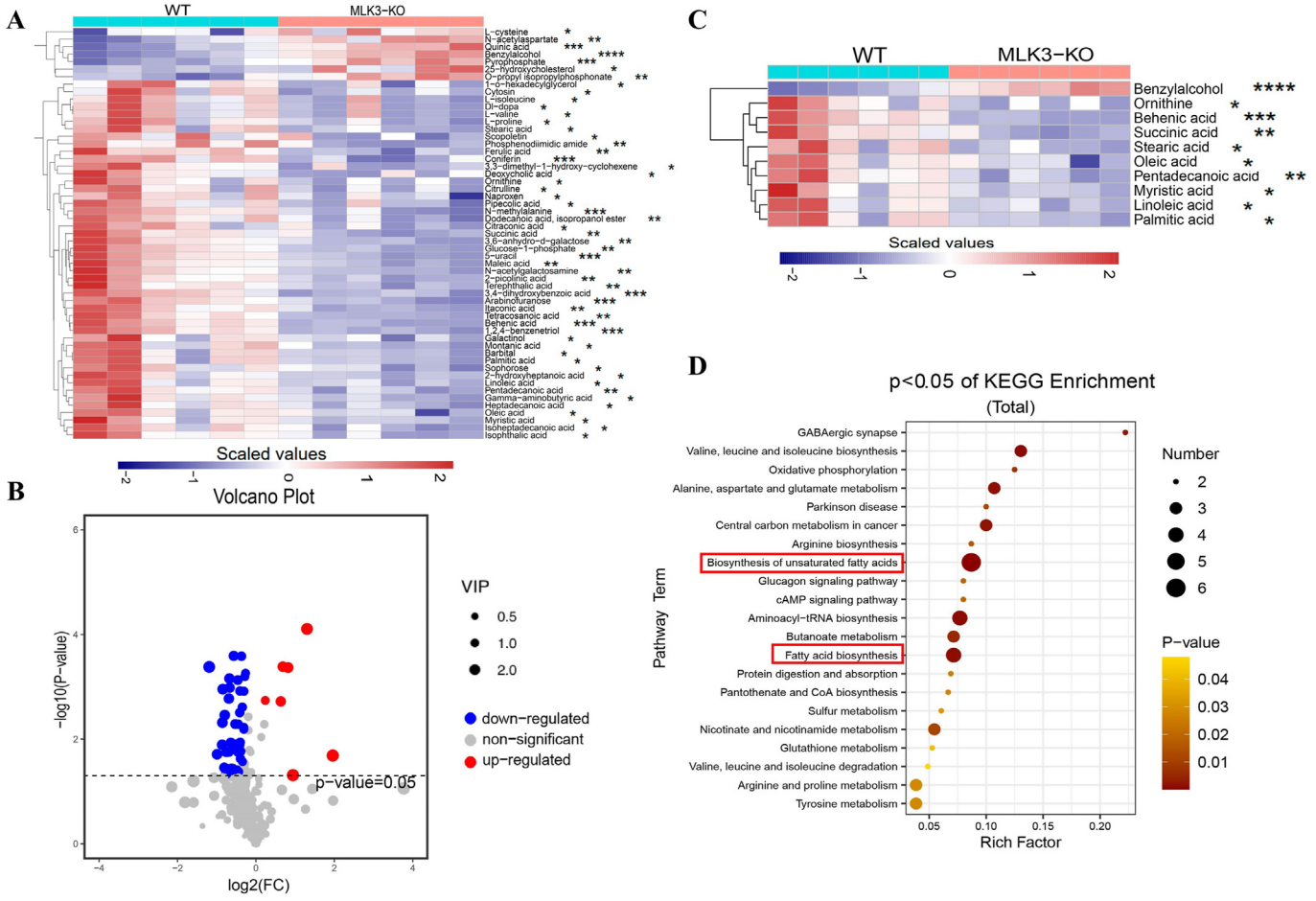

Figure 1. Bone metabolomic profiling between MLK3 KO and WT mice. A, All identified metabolites in a heat map. B, The deferentially expressed metabolites in volcano plot. The up-regulated metabolites are indicated in red, and the down-regulated ones are in blue. C, The representative bone-related metabolites. D, The enriched signaling of these metabolites by KEGG enrichment analyses. Student's t test was used to determine the significance. *, $P < 0.05$; **, $P < 0.01$; ***, $P < 0.001$.

2.10. Bone histomorphometry and immunohistochemistry (IHC) staining

The samples were initially fixed in 4% paraformaldehyde for 24 h, followed by decalcification in 14% EDTA solution for 2 weeks. After being embedded in paraffin, the samples were sectioned into 5 μm sagittal sections and subjected to hematoxylin and eosin (HE) staining. IHC staining was performed according to the standard protocol. Briefly, sections were incubated with primary antibodies of osteocalcin (OCN, 1:100, abcam13418) overnight at 4 °C. Subsequently, we used HRP-labeled secondary antibodies at room temperature for 1 h. DAB was used for IHC signal detection, then counterstaining with hematoxylin. The positive-stained cell was captured using the scanning system of the digital pathological section (Pannoramic MIDI).

2.11. Statistical analysis

At least triplicates were taken in each experiment, and all the data were expressed as mean ± SD. Data were analyzed by Student's t-test or One-way ANOVA (GraphPad Prism 8), and $P < 0.05$ was considered to be statistically significant.

3. Results

3.1. Imbalanced bone metabolism was found in MLK3 KO mice

To characterize the functional role of MLK3 in bone metabolism, a global metabolomic profiling between femurs derived from KO and WT mice was carried out. 55 metabolites were identified, of which nearly 40 metabolites were recognized with differential expression in these KO mice (Fig. 1A–B). Among these metabolites, the benzyl alcohol, oleic acid, behenic acid, ornithine, pentadecanoic acid, linoleic acid, succinic acid, stearic acid, palmitic acid and myristic acid were the most changeable metabolites between WT and KO mice (Fig. 1C). We found most of them were fatty acids, and KEGG enrichment also showed the metabolites were enriched in biosynthesis of unsaturated fatty acids and fatty acids (Fig. 1D), suggesting the abnormal lipid metabolism in MLK3 −/− mice.

3.2. Abnormal bone tissues and impaired bone quality were observed in MLK3 KO mice

To investigate the actual function of MLK3 in bone formation, we compared the bone tissues of KO mice and that of WT mice. By micro-CT examination, the representative 3D images of femurs showed the lower bone mass in the cortical bone and in trabecular bone (Fig. 2A). The quantification assays recorded the significant decreases in bone volume/total volume (BV/TV), bone volume (BV), bone mass density (BMD), trabecular thickness (Tb.Th), trabecular number (Tb.N) and an increase in trabecular separation (Tb.Sp) in KO mice (Fig. 2B). Furthermore, hematoxylin-eosin (H&E) staining of femurs showed that the thinner growth plate, less smooth edge of cortical bone and less paralleled alignment of osteocytes in KO mice (Fig. 2C), indicating more bone lost in KO mice.

3.3. Delayed fracture healing was found in KO mice

We next established a mouse femoral fracture model to compare the healing process of bone fracture between MLK3−/− and WT mice. The

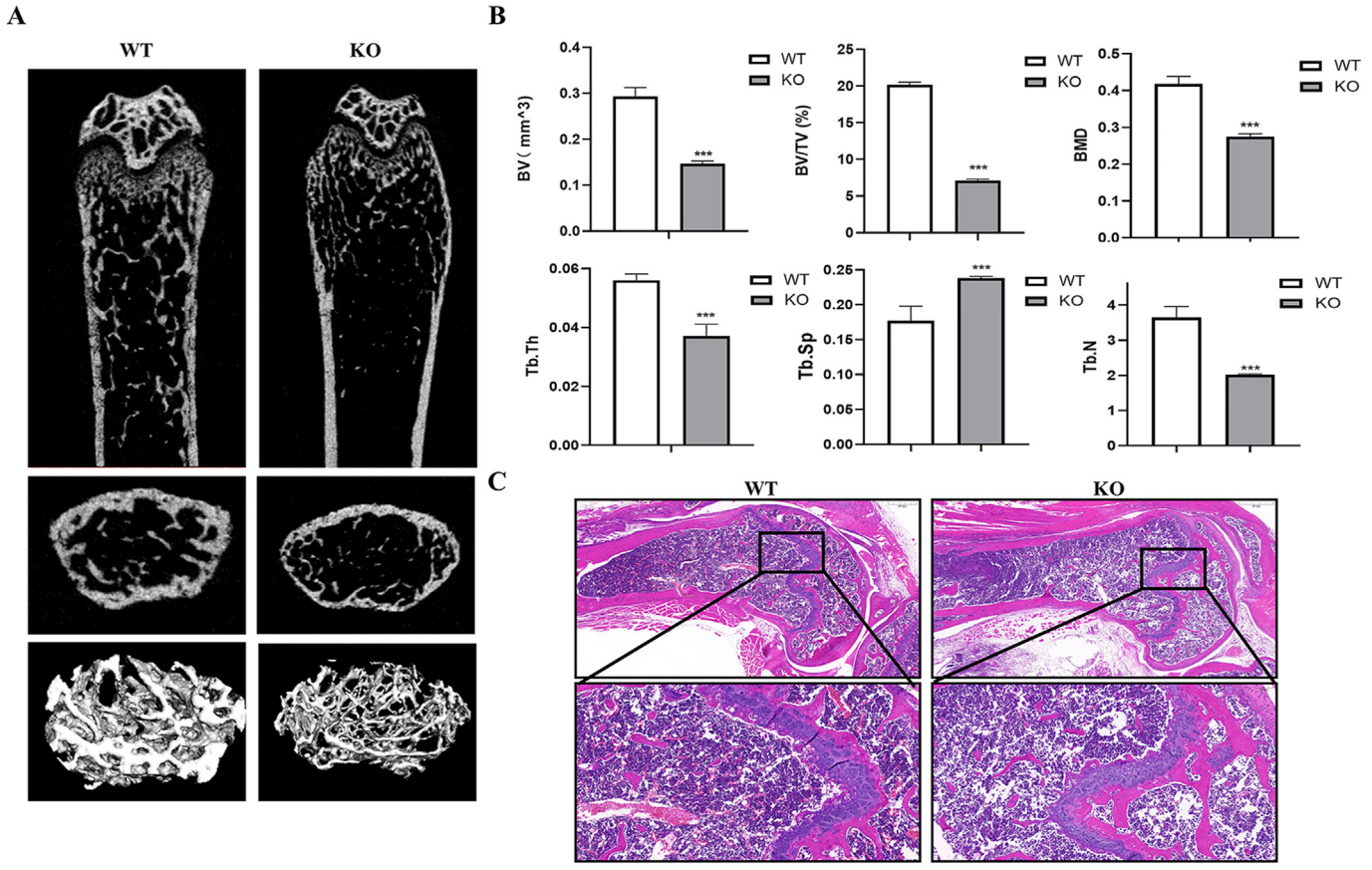

Figure 2. The impaired bone quality in MLK3 KO mice. A, 12-week-old WT and KO mice were sacrificed, and femurs were obtained for micro-CT assessment. The representative 3D images of cortical bone and the trabecular bone were shown. B, Quantification assays of the bone volume/total volume (BV/TV), bone volume (BV), bone mass density (BMD), trabecular thickness (Tb.Th) and trabecular number (Tb.N) and trabecular separation (Tb.Sp). C, Hematoxylin-eosin (H&E) staining of femurs from KO mice and WT mice. Student's t test was used to determine the significance. n = 6; *, $P < 0.05$; **, $P < 0.01$; ***, $P < 0.001$.

healing process was assayed by X-ray examination, and the representative images showed a poor healing effect was observed in KO mice compared with WT mice during the healing process (Fig. 3A). At week 4, a noticeable gap was observed in the KO group while it almost disappeared in WT group, indicating that the fracture healing process was delayed in KO mice. The 3D reconstructed images of μCT also confirmed the lower bone mass in the KO mice at week 4 (Fig. 3B) and week 6 (Fig. 3C), and the quantitative analyses showed MLK3 −/− mice had a significant decrease in BV/TV at week 4 and week 6, suggesting less newly formed mineralized bone in this KO mice (Fig. 3D–E). H&E staining of fracture healing position revealed that more osteocytes were enriched in the fracture sites of the WT group and the bone regeneration was more vigorously compared with the KO group (Fig. 3F). And the further IHC staining showed the decreased expression of osteocalcin (OCN) in the MLK3 KO group (Fig. 3G, Supplementary Fig. S1), which suggests an impaired effect of MLK3 KO on bone formation.

3.4. Osteogenic differentiation was suppressed in MSCs derived from MLK3 KO mice

Previous study demonstrated that MLK3 regulated osteoblast yet had no influence on osteoclast [12]. We next investigated the potential of MLK3 in osteoblast differentiation. Under osteogenic induction, the early marker of osteogenesis, ALP activity was lower in MLK3−/− MSCs at day 7 by qualitative and quantitative analyses (Fig. 4A). And fewer mineralized nodules were observed at day 14 in the MLK3 deficient MSCs when compared with the WT MSCs by ARS staining (Fig. 4B). Furthermore, several master regulators of osteogenesis including Runt-related transcription factor 2 (Runx2), ALP, OCN, osteopontin (OPN), Osterix (OSX) and bone morphogenetic protein 2 (BMP2) were found to be significantly downregulated by loss of MLK3 at day 9 (Fig. 4C).

A classical MLK3 inhibitor URMC-099 was further used to examine the *in vitro* effect of MLK3 on osteoblasts. It was introduced into mouse bone marrow MSCs, and the cell viability was examined. As shown in Supplementary Fig. S2, URMC-099 even with 100 nm only slightly suppressed cell growth at 96 h, suggesting it has low cytotoxicity. The concentration of 10 nm was introduced into MSCs for the osteogenic induction. The results showed that ALP activities were suppressed by this inhibitor at day 7 (Fig. 4D), and calcium nodules were also reduced at day 14 as well (Fig. 4E). The expression of osteogenic marker genes were also significantly suppressed by this inhibitor (Fig. 4F). All these data suggest that MLK3 promotes the osteogenesis of MSCs, and thereby stimulates

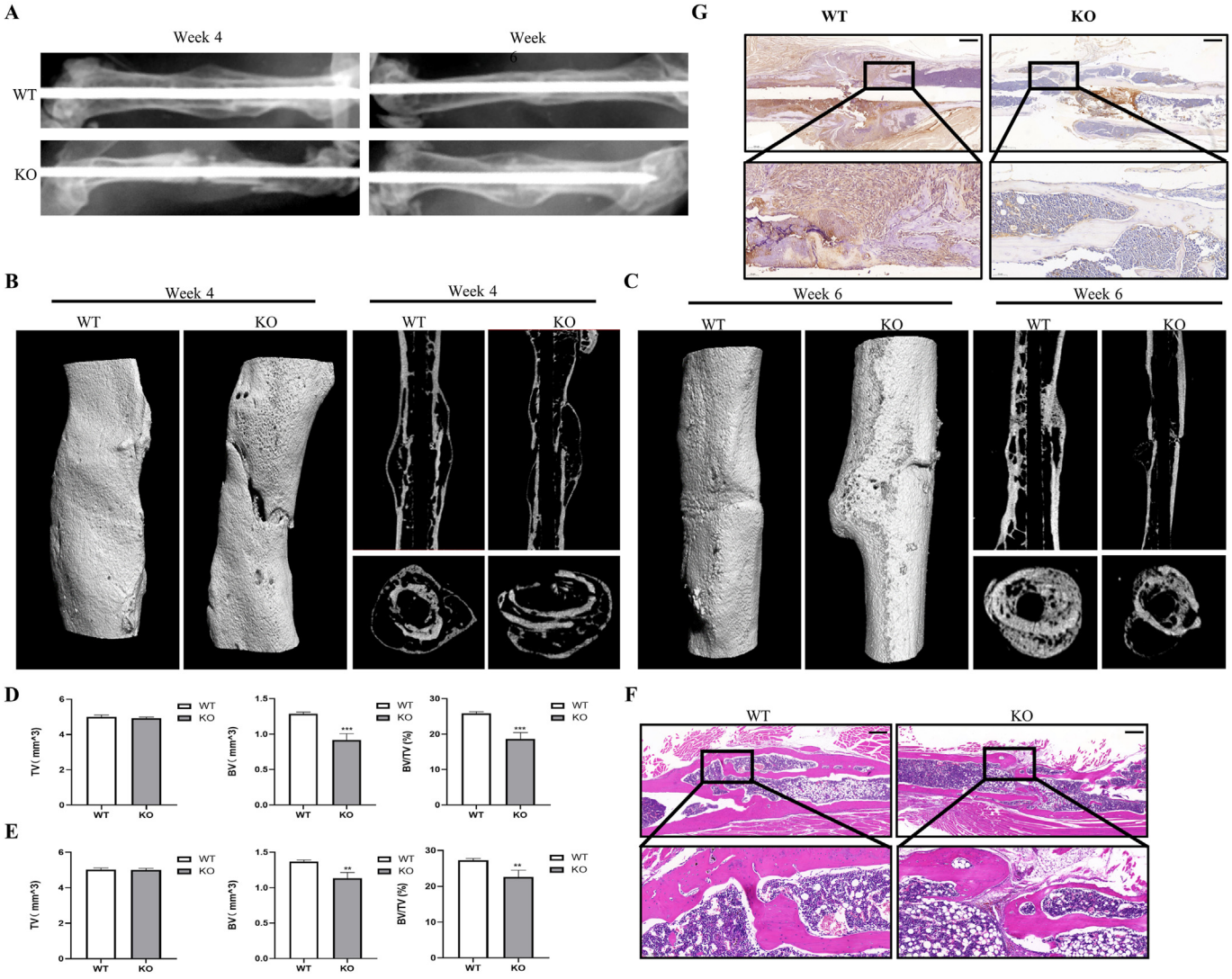

Figure 3. Delayed fracture healing in MLK3 KO mice. A, Representative images of the fracture healing process at week 4 and week 6 post-surgery by X-ray radiography. B-E, The representative 3D reconstructed images of micro-CT at week 4 (B) and week 6 (C) post-surgery. Quantitative analyses of bone volume (BV), total volume (TV) and bone volume/total volume (BV/TV) at week 4 (D) and week 6 (E). F-G, Representative images of Hematoxylin-eosin (H&E) staining (F) and immunohistochemistry staining (G) for OCN at week 6. Student's t test was used to determine the significance. n = 3; *, $P < 0.05$; **, $P < 0.01$; ***, $P < 0.001$.

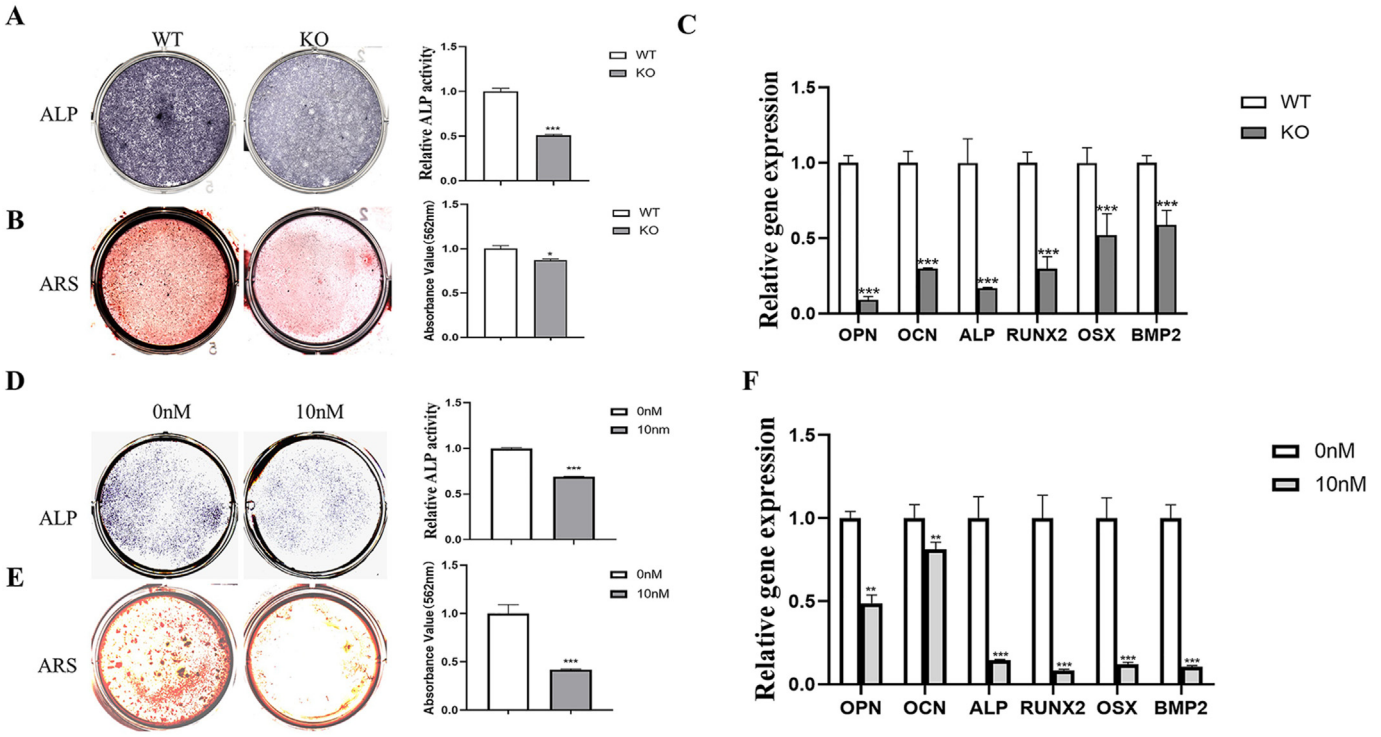

Figure 4. Inhibition of MLK3 suppressed the osteogenic differentiation of MSCs. A-C, MSCs were isolated from WT and MLK3 KO mice, and induced to the osteogenic differentiation. The quantitative analysis of ALP staining were examined at day 7 (A). The qualitative and quantitative analyses of ARS staining were measured at day 14 (B). And several osteoblast related genes were evaluated by qPCR examination (C). D-E, URMC-099, a classical MLK3 inhibitor, was applied to suppress MLK3 expression and its effect on osteogenesis was examined. ALP staining at day 7 (D) and ARS at day 14 (E) and the expression of several osteogenic marker genes (F) were assessed. All experiments were repeated at least three times. Student's t test was used to determine the significance. *, $P < 0.05$; **, $P < 0.01$; ***, $P < 0.001$.

bone formation.

3.5. MLK mediated osteogenic differentiation via MAPK signaling

To better understand which signaling cascades are involved in the MLK3 mediated osteoblast, we compared the transcriptome alteration between the femurs derived from KO and WT mice. Bioinformatics analyses of the RNA-seq data indicated that 226 genes were successfully identified (Fig. 5A). Of which, 169 genes (74.8%) were markedly up-regulated, whereas 57 genes (25.2%) were down-regulated in MLK3 KO mice (Fig. 5B). The characteristics of all identified genes were summarized, and several signaling pathways were affected in MLK3 −/− mice (Fig. 5C). Among them, MAPK signaling was the most remarkable signaling in the GSEA, and it was chosen for further validation. MAPK include ERK, p38, and JNK subfamilies, and we examined their expression in the MSCs derived from WT and KO mice at day 7 and 14 under osteogenic inductive condition. The results showed that no differences in the expression of ERK and JNK were observed in WT and MLK3 −/− MSCs, while their phosphorylated expression, including p-ERK, p-JNK and p-P38 was all suppressed in the MSCs with MLK3 absence at day 7 and day14 (Fig. 5D–F).

4. Discussion

Fracture is a conventional disease and it needs a long time to recover [21]. Delayed healing and nonunion frequently occur in a small portion of patients, which represents enormous burdens to patients and the social healthcare system [21,22]. Identifying the potential targets to facilitate fracture healing have great clinical significance. Osteoblasts are derived from MSCs and they are the primary cell type responsible for bone formation. Promoting the potential of osteoblast differentiation may be a promising strategy for bone formation. MLK3 is a member of the serine/threonine MAP3K family, and a previous study reported that MLK3 promoted osteogenesis and loss of MLK3 inhibited skeletal mineralization [12]. Our results revealed that MLK3 absence impaired bone quality, delayed fracture healing process as well as suppressed osteogenesis. We thus considered that MLK3 might be a potential therapeutic target to stimulate bone formation and accelerate fracture healing.

As a MAPK activator, MLK3 has been involved in various cell biological activities and disease progression such as cell death, immune responses, tumorigenesis et al. [10,11,17–19]. For instance, MLK3 silence induced cervical cancer cell apoptosis via the Notch-1/autophagy network [23]; MLK3 promoted melanoma proliferation and invasion through targeting microRNA-125 b [24], and it also targeted microRNA-520 b to regulate liver cancer cell migration [25]. MLK3 inhibitor was also reported to mediate pyroptosis to attenuate inflammation and cardiac dysfunction [26]. MLK3-deficient mice have attenuated JNK activation and induced metabolic dysfunction with a high-fat diet [27,28]. Although MLK3 has been reported to promote osteogenesis and contribute to cranial bone development, its detailed function in bone fracture remains obscure. To validate the actual contribution of MLK3 in bone formation, the MLK3 genetic KO mouse was generated in the present study. In terms of the growing period of normal bone, 12-week-old adult mice were selected to investigate the bone development and establish the fracture model. The abnormal bone tissues and impaired bone quality were observed in these MLK3 −/− mice, and a delayed healing process was also found during bone fracture of the MLK3 deficient mice as well. Further *in vitro* examination showed that loss of MLK3 suppressed osteoblast differentiation, and the MLK3 classical inhibitor URMC-099 also inhibited osteogenesis. These results indicated that deficiency of MLK3 suppressed osteoblasts and inhibited bone formation, suggesting it may be a potential therapeutic target for bone repair. The information gained from this study may bring a bright insight into

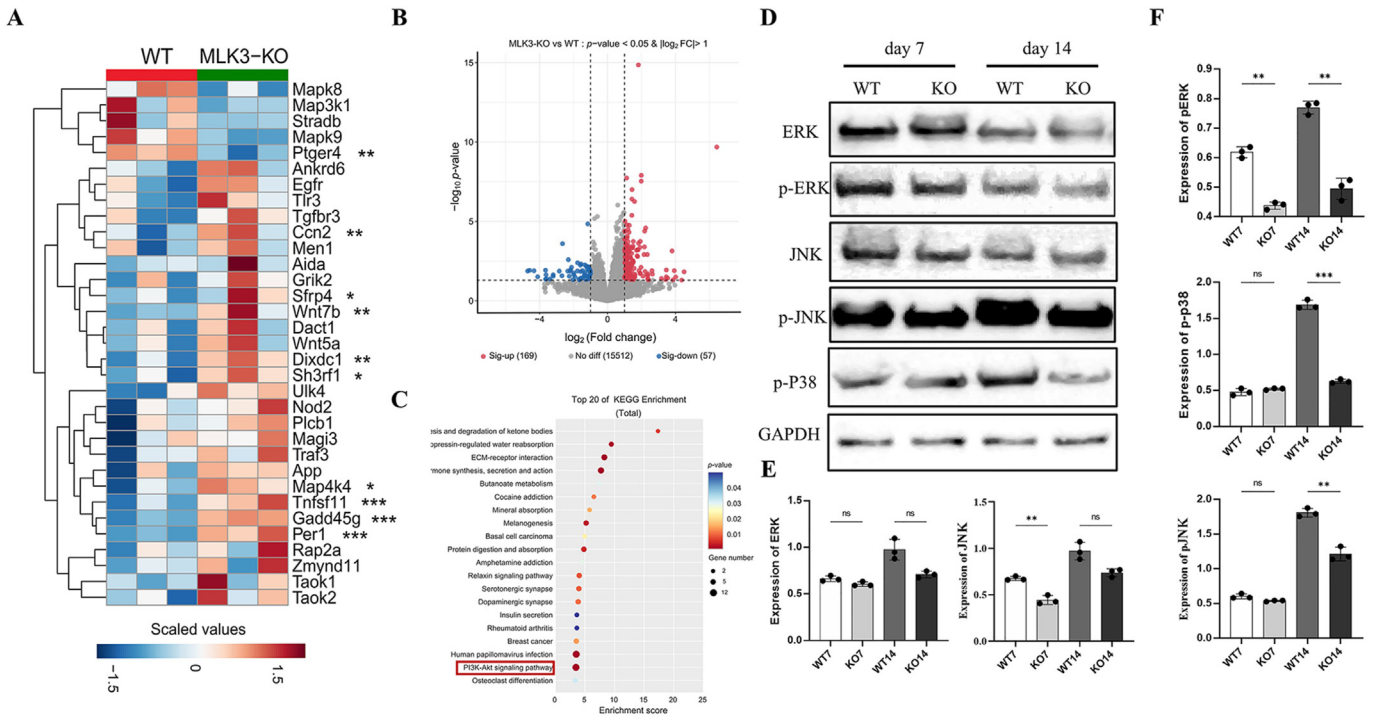

Figure 5. MAPK signaling was involved in the MLK3 mediated osteogenesis. A-C, RNA-sequencing studies of WT and KO mice was conducted, and the identified genes were shown in a heat map (A). Deferentially expressed genes were shown in the volcano plot (B). The enriched signaling of deferentially expressed genes. D-E, The expressions of MAPK signaling at the protein levels. The western blotting images of ERK, JNK, P38 and their phosphorylation in KO and WT groups (D), and quantification assays of ERK and JNK (E) as well as the phosphorylated ERK, JNK, P38 (F). One-way ANOVA was used to determine the significance. *, $P < 0.05$; **, $P < 0.01$; ***, $P < 0.001$.

developing an MLK3 activator as a therapeutic strategy for bone fracture.

Interestingly, MLK3-deficient mice exhibited metabolic dysfunction with a saturated fatty acid-enriched diet [27]. We wondered whether MLK3 participated in the bone metabolism. Using the femurs from WT and KO mice, global metabolomic profiling was carried out to identify the significant metabolites. 10 representative bone metabolites with different expression were identified as fatty acids, and KEGG analysis showed the biosynthesis of unsaturated fatty acids and fatty acids were enriched, which were closely correlated with osteogenic differentiation as previously reported [29]. For instance, free fatty acids could participate in osteoblast growth, differentiation, inflammation and apoptosis, and also activate peroxisome proliferator-activated receptor γ (PPARγ) and Runx2 to facilitate bone formation [36]. And polyunsaturated fatty acids also promoted bone formation by inducing prostaglandin E2 (PEG2) [29]. In the previous study of MLK3 −/− mice on a high-fat diet, non-alcoholic steatohepatitis (NASH) was protective against disease progression compared to the WT mice on the same diet, which suggested the involvement of MLK3 in lipid metabolism [16,28]. And our metabolomic profiling revealed that the biosynthesis of unsaturated fatty acids and fatty acids was significantly down-regulated in KO mice, which confirmed the above described conclusion.

MAPKs are a class of protein serine/threonine kinases that mediate intracellular signal transduction, and they play an essential regulatory role in cell growth, differentiation, and apoptosis [30,31]. As key players in skeletal development and bone homeostasis, MAPKs mainly affect osteoblast commitment and differentiation [18–20]. Of the three classic MAPKs, p38, ERK and JNK were all reported to determine the osteoblastic commitment and stimulate osteoblast differentiation [32–36]. MLK3 is a member of this gene family and has been implicated in multiple signaling cascades, including the NF-kappaB pathway, the extracellular signal-regulated kinase, JNK, and p38 MAPK pathways [37,38]. To clarify which signaling involved in the MLK3-mediated bone formation, a transcriptome profiling was performed to compare the differently expressed genes. Bioinformatics and GSEA analyses demonstrated that several signaling pathways were involved in the MLK3 KO induced bone formation. Of which, MAPK signaling pathway was the most remarkable signaling in this process. And our results of Western blotting demonstrated that JNK, ERK and p38 were significantly suppressed by loss of MLK3, indicating the MAPK signaling participated in the MLK3 mediated bone formation. However, there are some limitations in the present study, such as how MLK3 mediated MAPK signaling and bone metabolism. Further experiments to address these questions are needed in the near future.

In conclusion, our results demonstrated that deficiency of MLK3 suppressed osteogenesis *in vitro* and impaired bone formation and delayed fracture healing *in vivo*. By metabolomic and transcriptome profiling, abnormal bone metabolism and inactivation of MAPK signaling were identified in these KO mice. These results imply an essential role of the MLK3 signaling pathway in bone formation, and MLK3 therefore may be regarded as a novel therapeutic target for bone fracture.

Funding

This research did not receive any specific grant from funding agencies in the public, commercial, or not-for-profit sectors, and no material support of any kind was received.

Author contributions statement

Jin A.M., Zhang J.F. and Li Z.P. designed and supervised all the experiments; Yang X., Li Z.*P. and* Mai Y.X. conducted experiments and analyzed the data; Wei L., Peng L.Y., Pang F.X. and Wang L.J. provided the technical support; Yang X., Li Z.*P. and* Mai Y.X. prepared the manuscript. Zhang J.F. revised the manuscript. All authors reviewed and approved the manuscript.

Disclosure of potential conflicts

The authors declare that none of them have any conflict of interest.

Acknowledgments

We would like to thank Dr. Lingjun Wang for providing the MLK3 KO mice, and we also thank Xiaoxin Ye from OE Biotech Co., Ltd (Shanghai, China) for sequencing analyses.

Appendix A. Supplementary data

Supplementary data to this article can be found online at https://doi.org/10.1016/j.jot.2022.07.003.

References

[1] Leslie WD, Morin SN, Lix LM, Majumdar SR. Does diabetes modify the effect of FRAX risk factors for predicting major osteoporotic and hip fracture? Osteoporos Int : a journal established as result of cooperation between the European Foundation for Osteoporosis and the National Osteoporosis Foundation of the USA 2014; 25(12):2817–24.
[2] McGinty T, Mirmonsef P, Mallon PW, Landay AL. Does systemic inflammation and immune activation contribute to fracture risk in HIV? Curr Opin HIV AIDS 2016; 11(3):253–60.
[3] Tschirhart CE, Nagpurkar A, Whyne CM. Effects of tumor location, shape and surface serration on burst fracture risk in the metastatic spine. J Biomech 2004; 37(5):653–60.
[4] Makridis KG, Obakponovwe O, Bobak P, Giannoudis PV. Total hip arthroplasty after acetabular fracture: incidence of complications, reoperation rates and functional outcomes: evidence today. J Arthroplasty 2014;29(10):1983–90.
[5] Meals C, Meals R. Hand fractures: a review of current treatment strategies. J Hand Surg 2013;38(5):1021–31.
[6] Benjet C, Bromet E, Karam EG, Kessler RC, McLaughlin KA, Ruscio AM, et al. The epidemiology of traumatic event exposure worldwide: results from the World Mental Health Survey Consortium. Psychol Med 2016;46(2):327–43.
[7] Wiesel B, Nagda S, Mehta S, Churchill R. Management of midshaft clavicle fractures in adults. J Am Acad Orthop Surg 2018;26(22):e468–76.
[8] Rupp M, Biehl C, Budak M, Thormann U, Heiss C, Alt V. Diaphyseal long bone nonunions - types, aetiology, economics, and treatment recommendations. Int Orthop 2018;42(2):247–58.
[9] Zura R, Xiong Z, Einhorn T, Watson JT, Ostrum RF, Prayson MJ, et al. Epidemiology of fracture nonunion in 18 human bones. JAMA Surg 2016;151(11):e162775.
[10] Chadee D. Involvement of mixed lineage kinase 3 in cancer. Can J Physiol Pharmacol 2013;91(4):268–74.
[11] Chotirat R, Kathleen G. MLK3 signaling in cancer invasion. Cancers 2016;8(5):51.
[12] Zou W, Greenblatt M, Shim J, Kant S, Zhai B, Lotinun S, et al. MLK3 regulates bone development downstream of the faciogenital dysplasia protein FGD1 in mice. J. Clinic Invest 2011;121(11):4383–92.
[13] Kyriakis J. The integration of signaling by multiprotein complexes containing Raf kinases. Biochim Biophys Acta 2007;1773(8):1238–47.
[14] Gelbard H, Dewhurst S, Maggirwar S, Kiebala M, Polesskaya O, Gendelman H. Rebuilding synaptic architecture in HIV-1 associated neurocognitive disease: a therapeutic strategy based on modulation of mixed lineage kinase. Neurotherapeutics 2010;7(4):392–8.
[15] Handley M, Rasaiyaah J, Chain B, Katz D. Mixed lineage kinases (MLKs): a role in dendritic cells, inflammation and immunity? Int J Exp Pathol 2007;88(2):111–26.
[16] Hirsova P, Ibrabim S, Gores G, Malhi H. Lipotoxic lethal and sublethal stress signaling in hepatocytes: relevance to NASH pathogenesis. J Lipid Res 2016;57(10): 1–38.
[17] Kanthasamy A, Jin H, Mehrotra S, Mishra R, Kanthasamy A, Rana A. Novel cell death signaling pathways in neurotoxicity models of dopaminergic degeneration: relevance to oxidative stress and neuroinflammation in Parkinson's disease. Neurotoxicology 2010;31(5):555–61.
[18] Zhang X, Qin Q, Dai H, Cai S, Zhou C, Guan J. Emodin protects H9c2 cells from hypoxia-induced injury by up-regulating miR-138 expression. Braz J Med Biol Res 2019;52(3):e7994.
[19] Zhou D, Huang C, Lin Z, Zhan S, Kong L, Fang C, et al. Macrophage polarization and function with emphasis on the evolving roles of coordinated regulation of cellular signaling pathways. Cell Signal 2014;26(2):192–7.
[20] Zhang Z, Bai X, Zhang Z, Jin D. Establishment a closed femur fracture model with intramedullary nailing in mice. Acta Anat Sin 2012;43(1):135–8.
[21] Hak DJ, Fitzpatrick D, Bishop JA, Marsh JL, Tilp S, Schnettler R, et al. Delayed union and nonunions: epidemiology, clinical issues, and financial aspects. Injury 2014;45S:S3–7.
[22] Kostenuik P, Mirza FM. Fracture healing physiology and the quest for therapies for delayed healing and nonunion. J Orthop Res : Off Pub Ortho Res Soc 2017;35(2): 213–23.
[23] Ma L, Cheng Y, Zeng J. MLK3 silence induces cervical cancer cell apoptosis via the Notch-1/autophagy network. Clin Exp Pharmacol Physiol 2019;46(9):854–60.
[24] Zhang J, Lu L, Xiong Y, Qin W, Zhang Y, Qian Y, et al. MLK3 promotes melanoma proliferation and invasion and is a target of microRNA-125b. Clin Exp Dermatol 2014;39(3):376–84.
[25] Zhang F, Zhu Y, Wu S, Hou G, Wu N, Qian L, et al. MLK3 is a newly identified microRNA-520b target that regulates liver cancer cell migration. PLoS One 2020; 15(3):e0230716.
[26] Wang J, Deng B, Liu J, Liu Q, Guo Y, Yang Z, et al. Xinyang Tablet inhibits MLK3-mediated pyroptosis to attenuate inflammation and cardiac dysfunction in pressure overload. J Ethnopharmacol 2021;274:114078.
[27] Gadang V, Kohli R, Myronovych A, Hui DY, Perez-Tilve D, A aJ. MLK3 promotes metabolic dysfunction induced by saturated fatty acid-enriched diet. Am J Physiol Endocrinol Metab 2013;305(4):E549–56.
[28] Ibrahim SH, Gores GJ, Hirsova P, Kirby M, Miles L, Jaeschke A, et al. Mixed lineage kinase 3 deficient mice are protected against the high fat high carbohydrate diet-induced steatohepatitis. Liver Int : Off J Int Assoc Study Liver 2014;34(3):427–37.
[29] During A, Penel G, Hardouin P. Understanding the local actions of lipids in bone physiology. Prog Lipid Res 2015;59:126–46.
[30] Krens S, He S, Spaink H, Snaar-Jagalska B. Characterization and expression patterns of the MAPK family in zebrafish. Gene Expr Patterns : GEP 2006;6(8):1019–26.
[31] Tian Y, Wen H, Qi X, Zhang X, Li Y. Identification of mapk gene family in Lateolabrax maculatus and their expression profiles in response to hypoxia and salinity challenges. Gene 2019;684:20–9.
[32] Kim JH, Kim K, Kim I, Seong S, Nam KI, Kim KK, et al. Adaptor protein CrkII negatively regulates osteoblast differentiation and function through JNK phosphorylation. Exp Mol Med 2019;51(9):1–10.
[33] Matsuguchi T, Chiba N, Bandow K, Kakimoto K, Masuda A, Ohnishi T. JNK activity is essential for Atf4 expression and late-stage osteoblast differentiation. J Bone Miner Res : Off J Am Soc Bone Min Res 2009;24(3):398–410.
[34] Meng YC, Lin T, Jiang H, Zhang Z, Shu L, Yin J, et al. miR-122 exerts inhibitory effects on osteoblast proliferation/differentiation in osteoporosis by activating the PCP4-mediated JNK pathway. Mol Ther Nucleic Acids 2020;20:345–58.
[35] Greenblatt M, Shim J, Zou W, Sitara D, Schweitzer M, Hu D, et al. The p38 MAPK pathway is essential for skeletogenesis and bone homeostasis in mice. J. Clinic Invest 2010;120(7):2457–73.
[36] Marie P. Signaling pathways affecting skeletal health. Curr Osteoporos Rep 2012; 10(3):190–8.
[37] Thouverey C, Caverzasio J. The p38alpha MAPK positively regulates osteoblast function and postnatal bone acquisition. Cell Mol Life Sci : CMLS 2012;69(18): 3115–25.
[38] Song T, Zhang X, Yang GQ, Song Y, W C. Decrement of miR-199a-5p contributes to the tumorigenesis of bladder urothelial carcinoma by regulating MLK3/NF-κB pathway. Am J Transl Res 2015;7(12):2786–94.